



Simultaneous removal of tetracycline hydrochloride and As(III) using poorly-crystalline manganese dioxide



Huawei Wang^{a,c}, Daoyong Zhang^{a,b}, Shuyong Mou^a, Wenjuan Song^a, Fahad A. Al-Misned^d, M. Golam Mortuza^{d,e}, Xiangliang Pan^{a,*}

^a Xinjiang Key Laboratory of Environmental Pollution and Bioremediation, Chinese Academy of Sciences, Urumqi 830011, China

^b State Key Laboratory of Environmental Geochemistry, Institute of Geochemistry, Chinese Academy of Sciences, Guiyang 550002, China

^c University of Chinese Academy of Sciences, Beijing 100049, China

^d Department of Zoology, College of Science, King Saud University, Riyadh 11451, Saudi Arabia

^e Department of Zoology, Faculty of Life and Earth Science, Rajshahi University, Rajshahi 6205, Bangladesh

HIGHLIGHTS

- Tetracycline hydrochloride and As(III) were simultaneously oxidized by δ -MnO₂.
- Removal efficiency of TC and As(III) positively increased with initial δ -MnO₂ dosage.
- Competition between TC and As(III) for adsorption–oxidation sites occurs on δ -MnO₂ surface.

ARTICLE INFO

Article history:

Received 28 September 2014

Received in revised form 6 April 2015

Accepted 26 April 2015

Available online 15 May 2015

Keywords:

Antibiotics

Decomposition

Arsenic

Oxidation

Manganese dioxide

ABSTRACT

Simultaneous removal of antibiotic tetracycline hydrochloride (TC) and As(III) by poorly-crystalline Mn dioxide was investigated. TC and As(III) can be effectively oxidized and removed by MnO₂. High concentrations of TC and As(III) competed with each other for oxidation or adsorption sites on MnO₂ and thus affected their removal efficiency. The intermediates and products of TC after reaction with poorly-crystalline manganese dioxide were identified by LC–ESI–MS (liquid chromatography–electro spray ionization–mass spectrometry), and the decomposition pathways of TC by MnO₂ were proposed. This study is helpful for understanding the importance of environmental Mn dioxides in the decontamination of combined pollution by organic pollutants and metal(loid)s.

© 2015 Elsevier Ltd. All rights reserved.

1. Introduction

Arsenic (As) contamination in groundwater is a global health concern because of its high toxicity to humans (Bissen and Frimmel, 2003). It is estimated that more than 100 million people are at risk of As exposure through groundwater contamination (Ng, 2005). In Guizhou province, Inner Mongolia and Xinjiang Uighur autonomous regions of China, high levels of As in groundwater have been reported since the 1950s (Zhang et al., 2002; Rodriguez-Lado et al., 2013). In Kuytun area of Xinjiang, As concentrations in groundwater were 35 times more than the limit value for As set by the World Health Organization (WHO) (Li et al., 2008). In these contaminated sites, As(III) is the predominant

species, which shows higher mobility and toxicity than As(V) (Seyler and Martin, 1990).

The residents in arsenic contaminated areas are also unavoidably exposed to antibiotic pollution of groundwater. Most of the antibiotics, which are widely used in humans, animals and plants for preventing bacterial or fungal infections (Kummerer, 2009; Davies and Davies, 2010), are excreted via urine or faeces into surface water and groundwater (Alcock et al., 1999). In the rural arsenic contaminated areas, livestock wastewater and domestic sewage containing antibiotics are frequently used for irrigation of farmland, which can easily cause antibiotic pollution of soil and groundwater (Seyler and Martin, 1990; Guo et al., 2001; Barber et al., 2009; Buerge et al., 2009; Zhao et al., 2010). A variety of antibiotics (e.g., tetracycline, sulfamethoxazole and lincomycin) and their metabolites have been detected in groundwater in the northern China (Hu et al., 2010).

* Corresponding author.

E-mail address: panxl@ms.xjb.ac.cn (X. Pan).

Natural and artificial processes including adsorption, precipitation, hydrolysis and complexation (Seyler and Martin, 1990; Sassman and Lee, 2005; Ji et al., 2011; Yang et al., 2011; Liu et al., 2014) can affect transformation of antibiotics and arsenic, but these processes cannot thoroughly eliminate antibiotics from natural environments or reduce the mobility of arsenite in contaminated sites. Moreover, the environmental behaviors of antibiotics and arsenite correlate with each other. A recent study indicates that coexisted antibiotics in sediment have a strong effect on the biogeochemical cycle of As (Yamamura et al., 2014).

Poorly-crystalline manganese dioxides with structural disorder due to cation vacancies and random stacking arrangements are almost ubiquitous in a wide variety of geological settings (Post, 1999; Bodei et al., 2007; Bargar et al., 2009). They have strong ability in degradation of antibiotics (e.g., oxytetracycline, sulfamethazine and ciprofloxacin) (Zhang and Huang, 2005; Rubert and Pedersen, 2006; Gao et al., 2012), and oxidation and adsorption of heavy metals including As(III), Cr(III) and Co(II) (Lafferty et al., 2010a; Landrot et al., 2012; Crowther et al., 1983). The decrease of MnO₂ reactivity during oxidation of pollutants was also observed in recent studies (Lafferty et al., 2010a,b; Chen et al., 2011a). For example, Lafferty et al. (2010a) showed that As(III) oxidation by MnO₂ was rapid initially but the passivation phenomenon occurred on MnO₂ surface after several hours of reaction. Additionally, the co-solutes (substituted phenols) can significantly decrease the oxidation rate of chlortetracycline by MnO₂ (Chen et al., 2011a). However, the interactive effects of arsenic and antibiotics on their removal by MnO₂ are poorly understood.

The aim of this study was to evaluate the simultaneous removal of tetracycline hydrochloride (TC) and As(III) using MnO₂. Their interactive effects of TC and As(III) on their removal were also examined. The intermediates in the decomposition of TC by MnO₂ were analyzed by LC–MS and possible pathways of TC degradation by MnO₂ were proposed.

2. Materials and methods

2.1. Preparation of MnO₂ and TC solutions

Poorly-crystalline MnO₂ which has high reactivity (Tebo et al., 2004) was freshly synthesized (Villalobos et al., 2003) and confirmed by X-ray diffraction (XRD). The XRD data were taken from 5° to 80° (2θ). The sample sprayed with Au was analyzed by scanning electron microscopy (SEM) (Zeiss Super 55VP, Germany)-energy dispersive spectroscopy (EDS) (Bruker XFlash 5010, Germany). The particle size distribution and zeta potential were determined by a Malvern Zetasizer Nano analyzer (Malvern,

UK). The XRD spectrum, zeta potential, SEM micrograph with EDS spectrum and particle size of the synthesized MnO₂ were shown in Fig. S1. The XRD spectrum showed two main peaks at 37° and 66° belonged to MnO₂ (He et al., 2012; Lafferty et al., 2010a; Landrot et al., 2012). The MnO₂ particles had an average particle size of 180 nm and were negatively charged at various pHs (3.3–10.0), which was consistent with Murray's report (Murray, 1974). The EDS spectrum showed that the synthesized MnO₂ was predominantly composed of O and Mn with a little of Na and K.

Tetracycline hydrochloride (AR) was purchased from Hefei BoMei Biotechnology Co. Ltd, China. Sodium arsenite (AR) was obtained from Xiya Reagent Co. Ltd, China. Stocking solutions of 1 mM TC and As(III) were separately prepared in Milli-Q water and stored at 4 °C in the dark. Speciation of TC in solution at pH 1–13 based on the pK_a was shown in Fig. S2.

2.2. Batch experiments

Batch experiments for evaluation of TC and/or As removal by MnO₂ were conducted in 100 mL (working volume) Erlenmeyer flasks on a reciprocating shaker at 150 rpm and 30 °C. Briefly, various proportions of MnO₂ suspension (0–200 mg L⁻¹), TC (0–100 μM) and As(III) (0–125 μM) solutions were mixed together for reaction (Table 1). Before addition of TC and/or As(III) solution(s), the MnO₂ suspension was magnetically stirred at 500 rpm for at least 12 h to homogenize MnO₂ (Chen et al., 2011a). Table 1 listed the initial concentrations of MnO₂, TC and/or As(III) for batch experiments. The background electrolyte was 0.01 M NaCl and pH of all test solutions was adjusted to 6.0 using 0.01 M NaOH or HCl because the groundwater and surface water polluted with arsenic or antibiotics were usually found at neutral pHs (6–8) (Postma et al., 2007; Kummerer, 2009). At different time intervals (0, 10, 20, 30, 45, 60, 90, 150, 300 and 480 min), 1 mL of water samples were collected and filtered through 0.22 μm hydrophilic polyestersulfone membrane filters (Durapore PVDF, Millipore) for further analysis. Adsorbed TC was extracted by dissolving the membrane retained MnO₂ in 0.05 M hydroxylamine chloride for 0.5 h. All experiments were done in triplicate. All glassware was soaked overnight in K₂CrO₇–H₂SO₄ solution before use.

2.3. Analytical methods

TC concentration was measured using a Hitachi HPLC analyzer coupled with an ODS-C18 reversed chromatographic column (Waters, 4.6 × 250 nm, 5 μm) and an UV–DAD detector. The isocratic mobile phase was acetonitrile (35%, V/V)-0.01 M K₂HPO₄ (65%, pH 2.5, V/V) at 0.8 mL min⁻¹ and the UV-absorbance wavelength was 360 nm. The column temperature was 25 °C and injection volume was 20 μL. The retention time of TC was 4.05 min. The concentration range of TC standards was 0–80 μM (R² = 0.9999) and the detection limit of this method was 0.1 μM.

As(III) and As(V) in the water sample were separated by anion-exchange method (Tani et al., 2004). 100 μL of the sample solution was eluted through the Dowex 1 × 8 anion-exchange resin, where As(III) was eluted while As(V) was retained. The total As concentration in solution without anion exchange separation procedure and As(III) with anion exchange separation procedure were determined by hydride generation atomic fluorescence spectroscopy (HG-AFS) (AFS-810, Jitian, Beijing, China). As(V) concentrations were obtained by subtracting As(III) concentration from total As concentration. Soluble Mn(II) produced by the reductive dissolution of MnO₂ was determined by inductively coupled plasma-mass spectrometry (ICP-MS) (ELAN DRC II, PE, USA). The concentration range of Mn(II) standards was 0–20 μM (RSD = 2.54%) and the detection limit of this method was

Table 1
The initial concentrations of MnO₂, TC and/or As(III) for batch experiments.

Treatment	MnO ₂ (mg L ⁻¹)	TC (μM)	As(III) (μM)
A1	0	100	50
A2	20	100	50
A3	50	100	50
A4	100	100	50
A5	200	100	50
B1	100	100	0
B2	100	100	10
B3	100	100	50
B4	100	100	100
B5	100	100	125
C1	100	0	50
C2	100	10	50
C3	100	50	50
C4	100	100	50

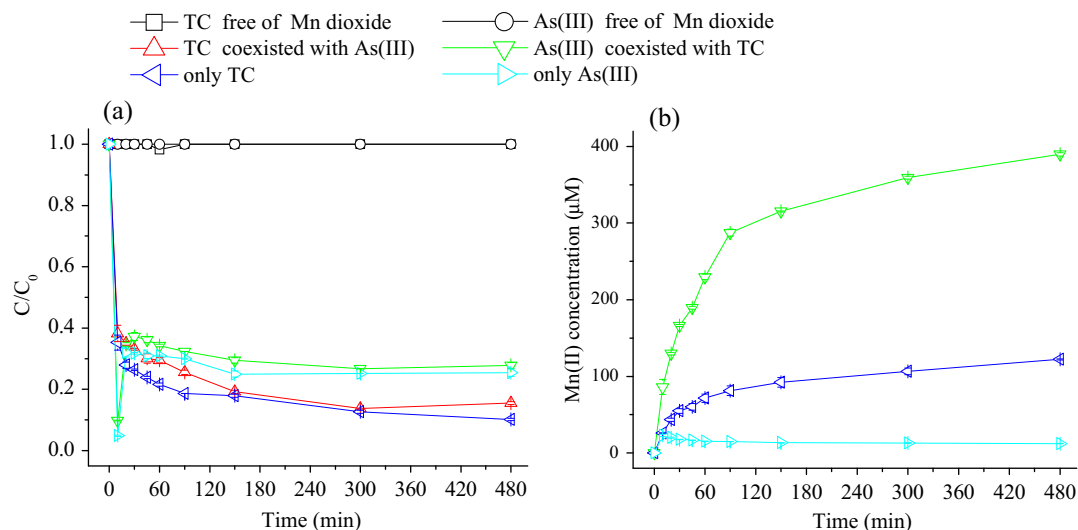


Fig. 1. (a) Percentage of TC and As(III) remaining in water as a function of reaction time with MnO_2 ; (b) Mn(II) concentration in water as a function of reaction time. The MnO_2 oxidative system, with 0.01 M NaCl as background electrolyte, had an initial MnO_2 concentration of 100 mg L^{-1} and an initial pH of 6.0. The initial TC and/or As(III) concentrations are $100 \mu\text{M}$ and/or $50 \mu\text{M}$, respectively. The MnO_2 oxidative experiments were performed at 150 rpm at 25°C .

$0.025 \mu\text{M}$. Solution pH was detected by an automatic potentiometric titrator with a pH electrode (Metrohm 702, Switzerland).

For identification of intermediate products of TC decomposed by MnO_2 , the supernatants were analyzed by liquid chromatography–electrospray ionization–mass spectrometry (LC–ESI–MS), including an ultra-HPLC (1200, Agilent, USA) and Quadrupole–linear ion trap mass spectrometer (4000QTRAP, AB Sciex, USA). Mass spectra were obtained with an electrospray ionization (ESI) source. The spectral resolution of the MS was 0.1 m/z . Before LC–MS analysis, the supernatants were centrifuged (6000 rpm, 10 min) and extracted by Poly-Sery HLB solid-phase extraction tubes (6 mL) (Shanghai ANPEL Scientific Instrument Co., Ltd.). The extracted intermediate product solution was eluted by 3 mL of methanol and subsequently flushed with high purity N_2 (99.999%) to dryness, and finally diluted with acetonitrile to 1 mL.

Means \pm standard deviations were calculated from three duplications ($n = 3$) and the significance between control and treatments was calculated using Tukey's test. The significance level was accepted when the value of p was <0.05 .

3. Results and discussion

3.1. Removal of TC and As(III) by MnO_2

In MnO_2 -free solutions, TC and As(III) concentrations changed slightly during the entire 480 min experimental time, indicating that air oxidation of As(III) and TC is limited. Oxidation of As(III) in pure water may need weeks (Pichler et al., 1999; Sorlini and Gialdini, 2010). Efficient removal of TC and/or As(III) was observed in all MnO_2 treatments (Fig. 1). At the initial stage (0–10 min), TC removal efficiency in the solutions containing TC alone was higher than that in the solutions containing both TC and As(III). A rapid removal of As(III) from solution was observed after 10 min of reaction. In the later stage (10–480 min), removal efficiency of TC or As(III) in the solutions containing TC or As(III) alone increased slowly with reaction time and was not significantly different from the solutions containing both TC and As(III). Additionally, oxidation of TC and As(III) led to reduction of solid Mn(IV) to free Mn(II) ion and its concentration increased with reaction time. Mn(II) concentration significantly increased when TC and As(III) coexisted in the

solutions. These results clearly indicated that MnO_2 was able to simultaneously remove TC and As(III) from water and the removal efficiencies of TC or As(III) were not significantly influenced even when both contaminants were present.

3.2. Effect of MnO_2 dosage on TC and As(III) removal

As seen from Figs. 2 and 3, in the TC and As(III) jointly contaminated system (TC–As(III) system), TC and As(III) were removed rapidly within the first 10 min and thereafter their removal rates were much lower with increasing reaction time. Their removal percentage was enhanced with increasing MnO_2 dosage but the removal efficiency decreased with increasing initial MnO_2 dosage when the sorption capacity (mg/g) is considered.

Ten min after the onset of the experiments, TC removal percentage was 26.8%, 38.5%, 61.8% and 78.7% in the presence of 20, 50, 100 and 200 mg L^{-1} of MnO_2 , respectively (Fig. 2). The kinetic data of TC oxidation or degradation by MnO_2 were fitted with the pseudo-first-order model (Eq. (1)):

$$\ln(C_t/C_0) = -kt \quad (1)$$

where k (min^{-1}) is the rate constant of the pseudo-first-order model; t (min) is the reaction time; C_0 (mg L^{-1}) is the initial concentration of TC, and C_t (mg L^{-1}) is the TC concentration at different reaction time.

The kinetics data were generally well fitted with the pseudo-first-order model ($R^2 = 0.67\text{--}0.93$) (Fig. S3a). The reaction rate constant k (Fig. 2b) increased from 0.000834 to 0.00279 with increasing initial MnO_2 dosage from 20 mg L^{-1} to 200 mg L^{-1} ($p < 0.05$). The positive dependence of oxidative transformation of tetracycline and other pollutants by dosage gradients of Mn dioxides has also been reported in previous studies (Chen et al., 2011a; Lu et al., 2011; Lu and Gan, 2013).

Removal of As(III) by MnO_2 was shown in Fig. 3a–d. The interaction between As(III) and MnO_2 showed two phases. In the first phase (0–10 min), fast removal of As(III) by MnO_2 was associated with the release of As(V). During the initial 10 min reaction, the As(III) removal efficiency was 83.3%, 90.2% and 92.2% at MnO_2 dosages of 50, 100 and 200 mg L^{-1} , respectively, indicating that As(III) was oxidized by MnO_2 or partially adsorbed onto MnO_2 surface. As(V) rapidly increased from zero to about 50% of the total As

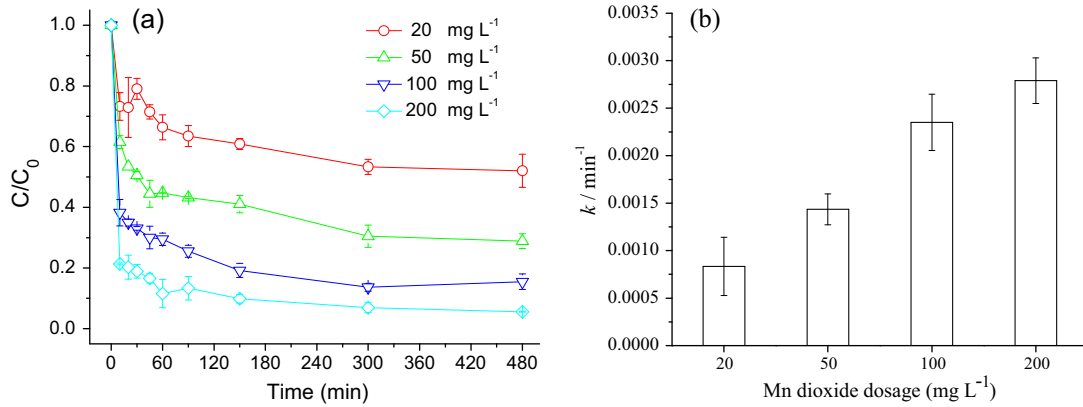


Fig. 2. (a) TC concentration in the water as a function of reaction time at various initial dosages of MnO_2 ; (b) the apparent rate constant k for TC removal by MnO_2 derived from the pseudo-first-order model. The initial experimental conditions: pH 6.0, $[TC]_0 = 100 \mu M$ and $[As(III)]_0 = 50 \mu M$.

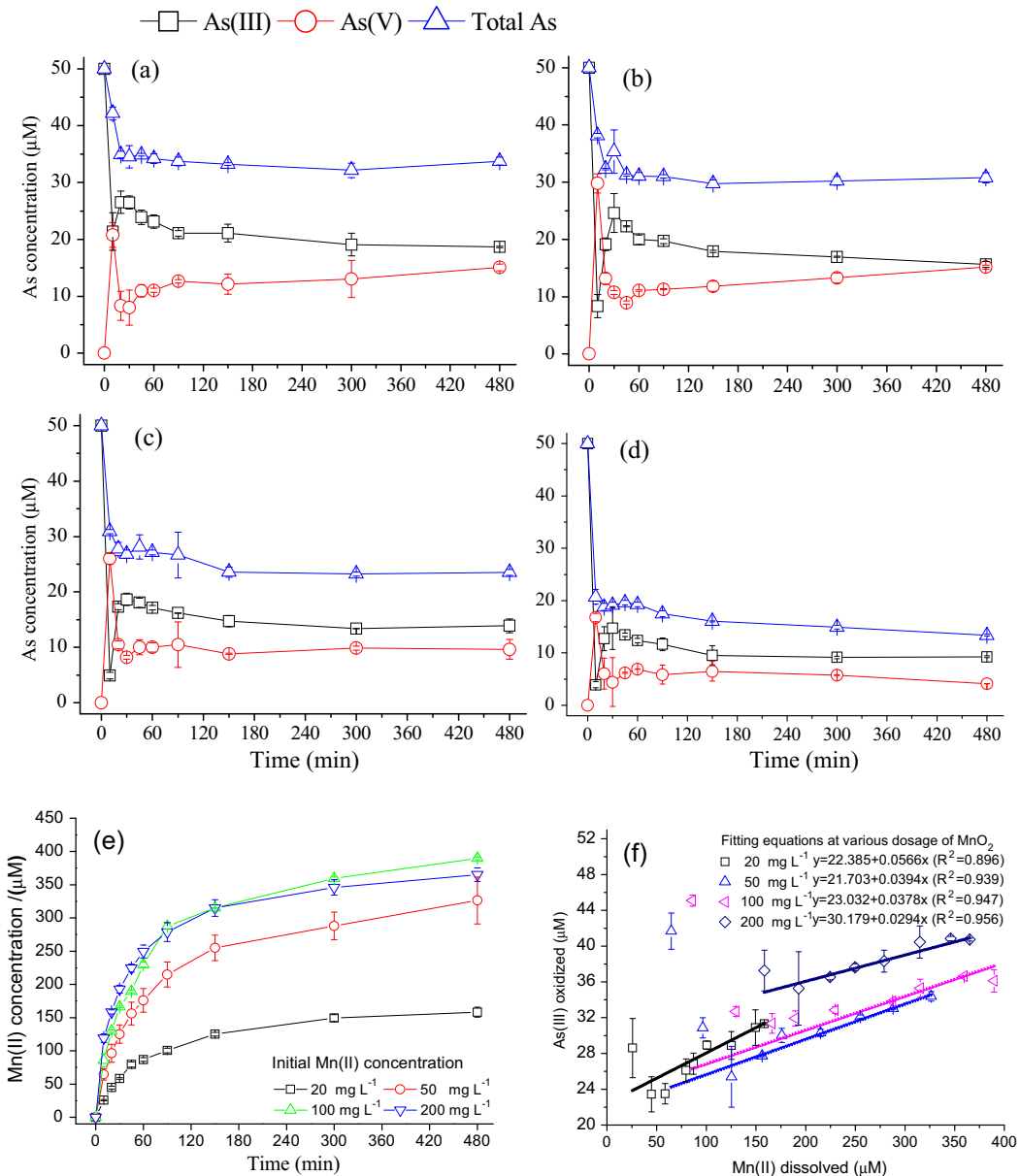


Fig. 3. Concentrations of As(III), As(V) and total As in water with reaction time at different dosages of MnO_2 ; (a) 20 $mg L^{-1}$ MnO_2 ; (b) 50 $mg L^{-1}$ MnO_2 ; (c) 100 $mg L^{-1}$ MnO_2 ; 200 $mg L^{-1}$ MnO_2 ; (e) Mn(II) concentration in solution with reaction time during oxidation of TC and As(III) by MnO_2 ; and (f) The correlation of the amount of As(III) oxidation with Mn(II) released during oxidation of TC and As(III) by MnO_2 . Initial experimental conditions: pH 6.0, TC concentration, 100 μM , and As(III) concentration, 50 μM .

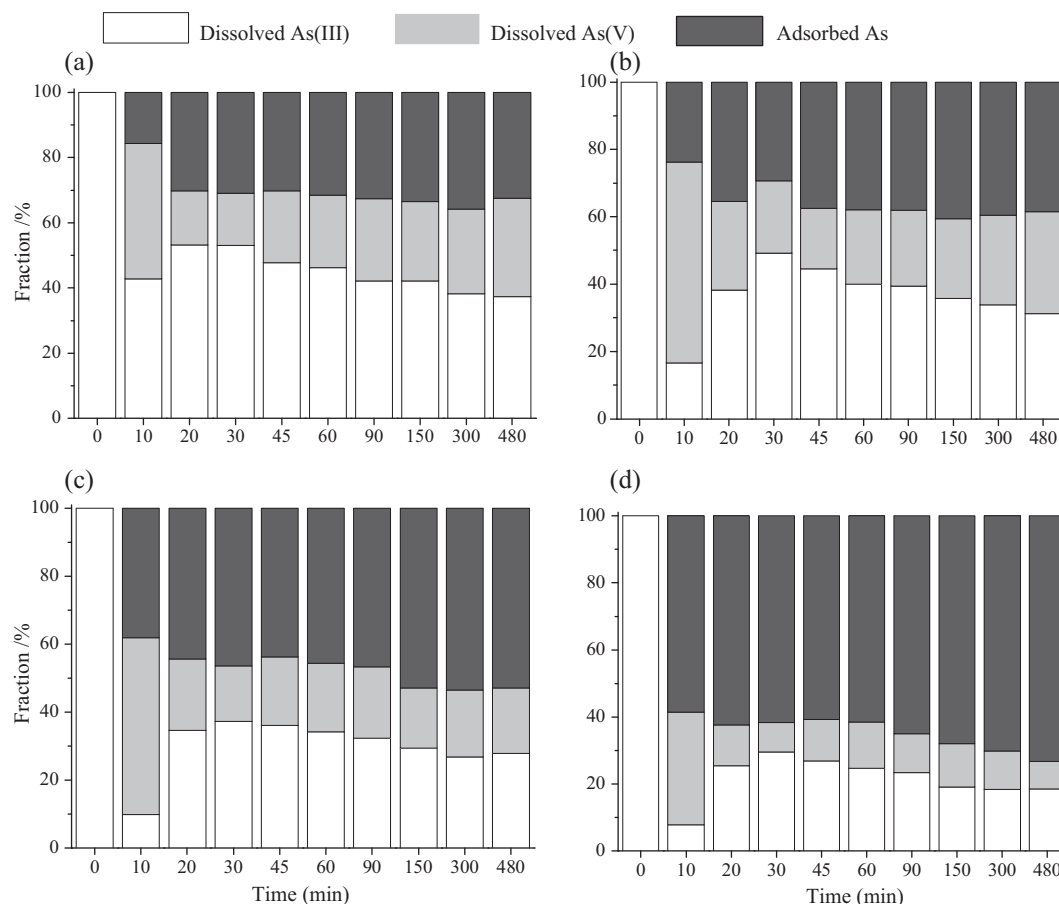


Fig. 4. Partition of dissolved As(III) and As(V) and the adsorbed As with reaction time at different dosages of MnO_2 . (a) $20 \text{ mg L}^{-1} \text{ MnO}_2$; (b) $50 \text{ mg L}^{-1} \text{ MnO}_2$; (c) $100 \text{ mg L}^{-1} \text{ MnO}_2$; (d) $200 \text{ mg L}^{-1} \text{ MnO}_2$; The initial experimental conditions: pH 6.0, an initial TC concentration of $100 \mu\text{M}$, and an initial As(III) concentration of $50 \mu\text{M}$.

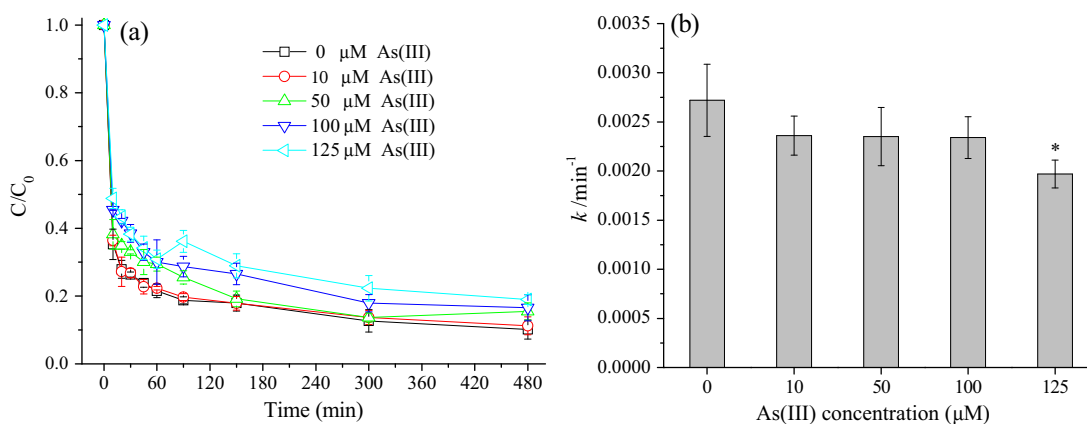


Fig. 5. (a) Effect of initial As(III) concentration on TC removal by MnO_2 ; (b) the apparent rate constant k for TC derived from the pseudo-first-order model. The initial experimental conditions: pH 6.0, $[\text{TC}]_0 = 100 \mu\text{M}$, $[\text{As(III)}]_0 = 0\text{--}125 \mu\text{M}$, and $[\text{MnO}_2]_0 = 100 \text{ mg L}^{-1}$.

at an initial MnO_2 of 20 mg L^{-1} and 78.2–84.1% of the total As at initial MnO_2 dosages of $50\text{--}200 \text{ mg L}^{-1}$ during the initial 10 min reaction (Fig. S3b). In the second phase (10–480 min), a slow As(III) oxidation and As(V) adsorption was observed, associated with the release of Mn(II) to solution (Fig. 3f), which indicates As(III) oxidation by MnO_2 . As(V) drastically dropped to 23.9%, 40.8%, 37.7% and 32.3% at 20 min at initial MnO_2 dosages of 20, 50, 100 and 200 mg L^{-1} , respectively and thereafter the proportion of As(V) in total As showed increasing trends during the rest

460 min (Fig. S3b). At initial MnO_2 dosages of $20\text{--}200 \text{ mg L}^{-1}$, oxidation of one molar As(III) to As(V) is accompanied with release of 17–34 molar free Mn(II) ions (Fig. 3f), which is the reductive product of MnO_2 . As(III) must be adsorbed to the Mn dioxide surface prior to oxidation, but only As(V) can be retained on the mineral surface (Manning et al., 2002; Lafferty et al., 2010a). Therefore, it is suggested that removal of As(III) from solution can be attributed to rapid adsorption and oxidation of As(III) to As(V) by MnO_2 and subsequent adsorption of As(V) to MnO_2 . The total As

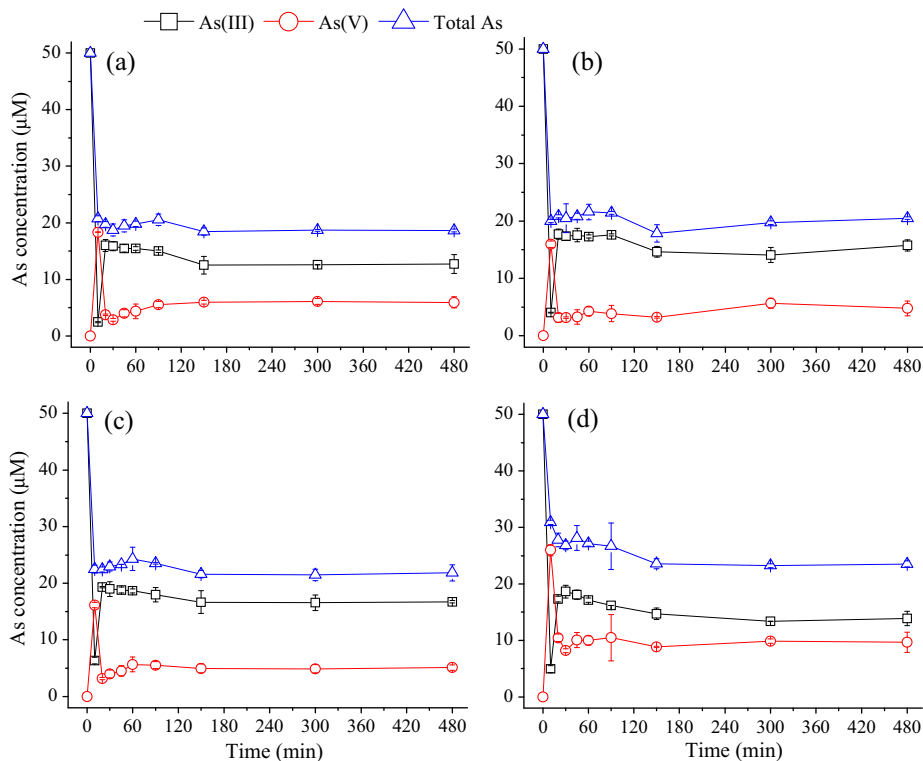


Fig. 6. The dissolved As(III), As(V) and total As concentrations with time in the presence of $100 \text{ mg L}^{-1} \text{ MnO}_2$ and various initial concentrations of TC. (a) $0 \text{ } \mu\text{M}$ TC, (b) $10 \text{ } \mu\text{M}$ TC, (c) $50 \text{ } \mu\text{M}$ TC, and (d) $100 \text{ } \mu\text{M}$ TC. Initial experimental conditions: pH 6.0, $[\text{As(III)}]_0 = 50 \text{ } \mu\text{M}$, $[\text{TC}]_0 = 0\text{--}100 \text{ } \mu\text{M}$, and $[\text{MnO}_2]_0 = 100 \text{ mg L}^{-1}$.

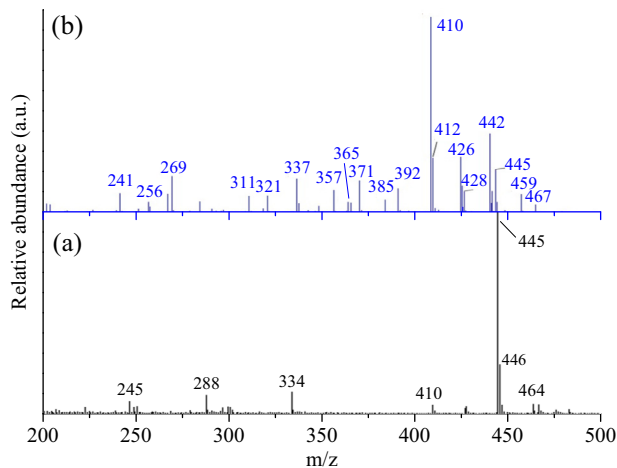


Fig. 7. (a) MS spectra of MnO_2 -free $100 \text{ } \mu\text{M}$ TC (control) and (b) possible intermediates of TC after 480 min of oxidation by $100 \text{ mg L}^{-1} \text{ MnO}_2$.

concentration in solution significantly decreased with increasing MnO_2 dosage (Fig. 3a–d) whilst adsorbed As increased with MnO_2 dosage (Fig. 4).

It was worth noting that the release of Mn(II) from MnO_2 to solution was accompanied by the simultaneous removal of TC and As(III) by MnO_2 . Meanwhile, decreasing reactivity of MnO_2 was observed in the TC and As(III) jointly contaminated system, which was mainly attributed to passivation of MnO_2 surface. MnO_2 is a poorly-ordered form of hexagonal birnessite, mainly with two types of reactivity sites: the vacancy sites within Mn(IV) octahedral layers and the edge sites at Mn(IV) octahedral layers edges (Drits et al., 1997; Lafferty et al., 2010a,b). It is reported that adsorption of As(III) and As(V) only occurs at the

edge sites while Mn(II) can be adsorbed at both the vacancy sites and the edge sites (Tournassat et al., 2002; Manning et al., 2002). Lafferty et al. (2010a) showed that decrease of MnO_2 reactivity was attributed to early adsorption of Mn(II) onto MnO_2 surface and subsequently formation of Mn(III)/Mn(IV) conproportionation. In this study, the large amount of Mn(II) in solution suggests that physically block of As(III) oxidation would occur due to fully or partially adsorption of Mn(II) at the vacancy sites and the edge sites of MnO_2 . As(V) adsorption at the edge sites also blocks As(III) oxidation (Tournassat et al., 2002). As shown in Fig. 4, only when MnO_2 dosage was as high as 200 mg L^{-1} , can the fraction of dissolved As(V) be decreased significantly. This implies that high dosage of MnO_2 may alleviate MnO_2 surface passivation phenomenon. Moreover, the inhibitory effect of adsorbed Mn(II) on reactivity of MnO_2 was also reported during the oxidation of other pollutants including chlortetracycline, octylphenol and nonylphenol (Chen et al., 2011a; Lu and Gan, 2013).

3.3. Effect of As(III) concentration on TC removal

It can be seen from Fig. 5a that the TC removal efficiency was significantly decreased in the presence of high concentrations of As(III) ($p < 0.05$). For example, after 10 min reaction, the TC removal efficiency was 64.7% in As(III) free solution but decreased to 60.4%, 54.5% and 51.1% in the presence of 50, 100 and $125 \text{ } \mu\text{M}$ As(III), respectively. When As(III) concentration was $125 \text{ } \mu\text{M}$, the rate constant k was 0.00272 ($R^2 = 0.727\text{--}0.955$), which significantly decreased in comparison with the control (0.00197 , $R^2 = 0.716\text{--}0.895$) (Figs. 5b and S4a). Effect of As(III) on the adsorption of TC onto MnO_2 surface was further examined (Fig. S5). Adsorbed TC accounted for a relatively small fraction (2.80–3.96%) of total TC removal. Compared with the control, the proportions of adsorbed TC in the presence of $125 \text{ } \mu\text{M}$ As(III) were not significantly different. These results suggest that the removal of TC is mainly due to

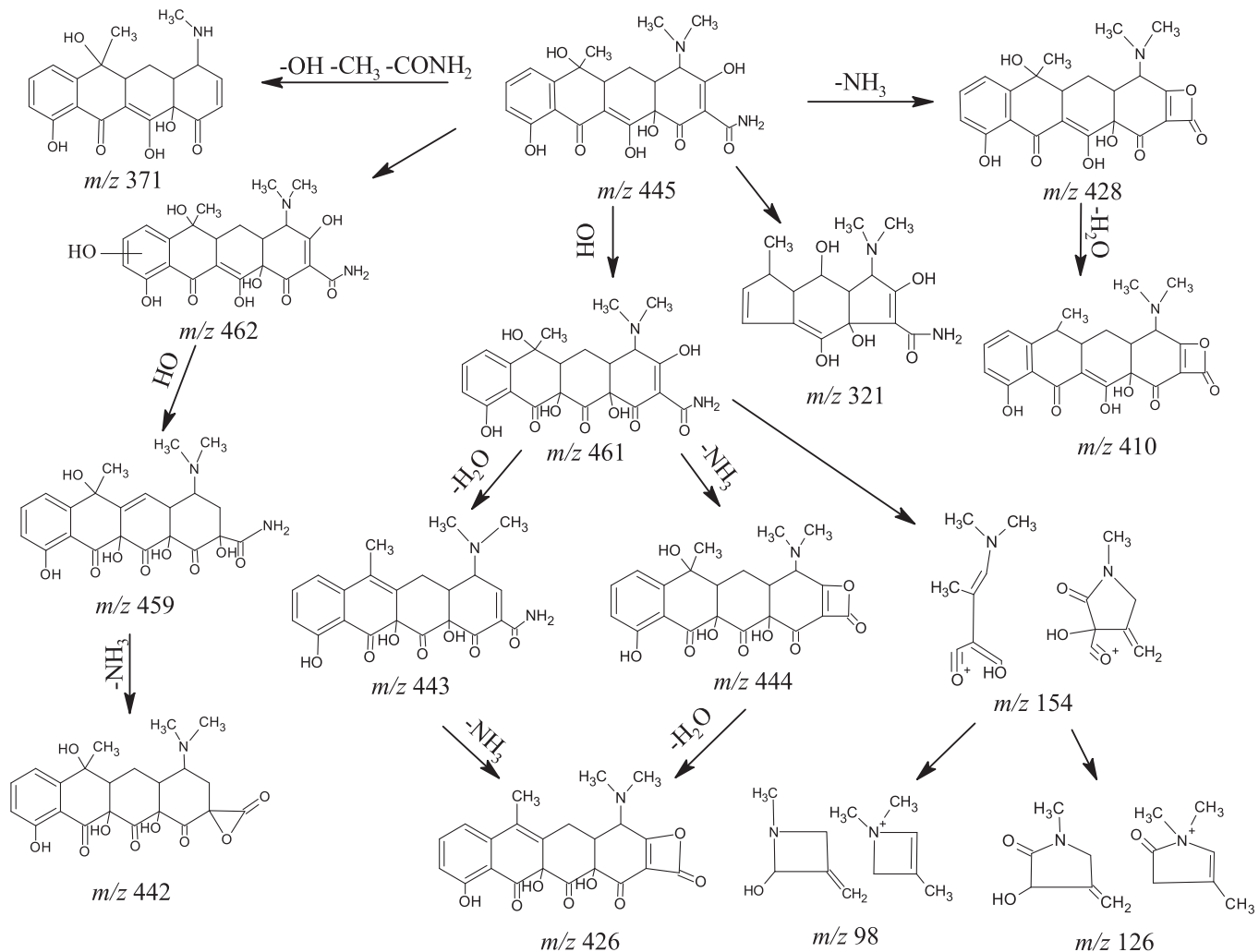


Fig. 8. Potential oxidation and degradation pathways of TC by MnO₂.

decomposition by MnO₂. Similar results were observed by other researchers (Chen et al., 2011a; Zhang et al., 2008).

The inhibition of TC removal by As(III) can be explained as follows. Firstly, when pH ranged from 3.3 to 7.7, TC mainly occurred as a neutral molecule (TCH₂) (Fig. S2). As(III) mainly occurs in the fully protonated form (H₃AsO₃) when pH is less than 9 (Sadiq, 1997) while MnO₂ is negatively charged. This means that protonated As(III) can be strongly adsorbed by negatively MnO₂ and this significantly inhibits adsorption and decomposition of TC by MnO₂. At early stages of reaction, the rapid occupation of MnO₂ surface reactivity sites by As(III) led to the decrease of TC reaction rate. For example, after 10 min of reaction, a rapid removal and oxidation of As(III) and a fast increase of As(V) concentration in solution were observed (Fig. 3). This implies the competition for reactive sites between TC and As(III). Moreover, the increased Mn(II) concentration in solution in the presence of various concentrations of As(III) (Fig. S4b) indicated that MnO₂ was consumed by dissolved As(III). Therefore, inhibitory effects on TC removal by As may also be related to the competitive adsorption of Mn(II) onto MnO₂ reactive sites.

3.4. Effect of TC concentration on As removal

Inhibitory effect of TC on the removal and oxidation of As(III) and adsorption of As(V) was shown in Fig. 6. Low concentrations

of TC were removed rapidly and thus the slight inhibition of As removal by TC was due to the depletion of TC by MnO₂. Higher concentrations of TC caused more inhibitory effects of TC on As removal ($p < 0.05$). After 10 min of reaction, total As concentration in solution decreased from initial 50.0 to 20.8 μM in absence of TC, while total As concentration increased by 48.1% compared to the control in the presence of 100 μM TC. The significant increase of release of Mn(II) into solution was observed in the presence of TC (Fig. S6), indicating that the depletion of MnO₂ by TC led to the decrease of As removal. This means that the inhibitory effect of high concentrations of TC on As(III) removal can be attributed to its competition with As(III) and As(V) for oxidative sites on MnO₂ surface. Furthermore, the complexation of amine and carbonyl in TC with Mn(II) through cation bridging may decrease the availability of MnO₂ (Tantuvay and Khan, 2004).

3.5. TC decomposition by MnO₂

The possible intermediate products or by-products of decomposition of TC by MnO₂ were identified from the ESI-MS spectra (Fig. 7), and the possible degradation pathways of TC by MnO₂ were proposed (Fig. 8).

The ion products at m/z 445 were designated as the tetracycline molecule (Dalmazio et al., 2007; Chen et al., 2011b). The intermediate with m/z 371 was generated due to losing N-methyl,

hydroxyl and amino groups of tetracycline molecule. This was in accordance with TC oxidation using potassium ferrate (Jiao et al., 2008) and photolysis of TC using luminescent bacteria (Ma et al., 2012). Moreover, the protonated tetracycline dissociates to mid mass ions at m/z 321 via loss of m/z 124 (Vartanian et al., 1998). Two additional ions at m/z 428 and 410 were obtained from the tetracycline molecule. Loss of *N*-methyl groups due to the low bond energy of N–C would generate product with m/z at 428, and this product was also identified during microbial degradation of oxytetracycline in sediments (Delepee et al., 2000). Further degradation would lead to the formation of m/z 410 via the loss of H₂O and structurally analogous ions. These findings confirm the results about degradation of TC by ozone (Dalmazio et al., 2007).

One of the by-products with m/z of 459 mainly originated from the H-abstraction reaction with the hydroperoxyl radical or oxidation of compound C to quinone (Jeong et al., 2010; Mboula et al., 2012). The by-product with the mass value of 442 resulted from the deamination of m/z 459. Four of the by-products with m/z of 461, 443, 444 and 426 were identified as oxidation products of the tetracycline molecule in this study and previous reports (Dalmazio et al., 2007; Jeong et al., 2010; Mboula et al., 2012). The intermediate with an m/z 461 was generated by the addition of a hydroxyl group on the phenol group of tetracycline molecule, and the results were also reported during photocatalytic decomposition of TC (Mboula et al., 2012). The by-products with m/z of 426 are due to the loss of H₂O and amino groups.

After the tetracycline molecule structure was destroyed, some small molecular intermediates were produced through the open-ring reaction and cleavage of the central carbon, and similar results were also observed during photocatalytic degradation of rhodamine B (Yu et al., 2009) and malachite green in TiO₂ suspensions (Ju et al., 2008). For example, the potential intermediates with an m/z of 154 originated from the precursor ions with m/z of 461. Then the fragment ions at m/z 154 dissociated to m/z 126 and m/z 98, and then the m/z 98 led to the generation of smaller products via the loss of water and CO units (Vartanian et al., 1998). Finally, CO₂, H₂O and inorganic ions can be generated by further oxidation steps.

4. Conclusions

This work demonstrates that MnO₂ is an effective material for simultaneous removal of TC and As(III) from water. Removal efficiency of TC and As(III) increased with increasing MnO₂ dosage. Removal efficiency of TC was affected by high concentrations of As(III) and the coexisting TC also competed for oxidation or adsorption sites on the surface of MnO₂ against As(III) and thus reduced the removal efficiency of As(III). ESI–MS analysis showed that intermediates of TC with different mass values were produced after reaction of MnO₂. These by-products mainly stemmed from TC degradation after losses of some groups from the ring or wreck of aromatic ring. This study is also helpful for understanding the behavior of arsenic and antibiotic in natural environments, where Mn dioxide is ubiquitous.

Acknowledgement

This work was supported by the National Natural Science Foundation of China (U1120302, U1403181, 21177127 and 41203088) and the West Light Foundation of Chinese Academy of Science (XBBS201304). Partial funding for this research was also received from the Visiting Professor Program at King Saud University, Riyadh, Saudi Arabia.

Appendix A. Supplementary material

Supplementary data associated with this article can be found, in the online version, at <http://dx.doi.org/10.1016/j.chemosphere.2015.04.070>.

References

- Alcock, R.E., Sweetman, A., Jones, K.C., 1999. Assessment of organic contaminant fate in wastewater treatment plants I. Selected compounds and physicochemical properties. *Chemosphere* 38, 2247–2262.
- Barber, L.B., Keefe, S.H., Leblanc, D.R., Bradley, P.M., Chapelle, F.H., Meyer, M.T., Loftin, K.A., Kolpin, D.W., Rubio, F., 2009. Fate of sulfamethoxazole, 4-nonylphenol, and 17 beta-estradiol in groundwater contaminated by wastewater treatment plant effluent. *Environ. Sci. Technol.* 43, 4843–4850.
- Bargar, J.R., Fuller, C.C., Marcus, M.A., Brearley, A.J., De la Rosa, M.P., Webb, S.M., Caldwell, W.A., 2009. Structural characterization of terrestrial microbial Mn oxides from Pinal Creek, AZ. *Geochim. Cosmochim. Acta* 73, 889–910.
- Bissen, M., Frimmel, F.H., 2003. Arsenic – a review. – Part 1: Occurrence, toxicity, speciation, mobility. *Acta Hydrochim. Hydrobiol.* 31, 9–18.
- Bodei, S., Manceau, A., Geoffroy, N., Baronnet, A., Buatier, M., 2007. Formation of todorokite from vernadite in Ni-rich hemipelagic sediments. *Geochim. Cosmochim. Acta* 71, 5698–5716.
- Buerge, I.J., Buser, H.R., Kahle, M., Muller, M.D., Poiger, T., 2009. Ubiquitous occurrence of the artificial sweetener acesulfame in the aquatic environment: an ideal chemical marker of domestic wastewater in groundwater. *Environ. Sci. Technol.* 43, 4381–4385.
- Chen, G., Zhao, L., Dong, Y.H., 2011a. Oxidative degradation kinetics and products of chlortetracycline by manganese dioxide. *J. Hazard Mater.* 193, 128–138.
- Chen, H., Luo, H.J., Lan, Y.C., Dong, T.T., Hu, B.J., Wang, Y.P., 2011b. Removal of tetracycline from aqueous solutions using polyvinylpyrrolidone (PVP-K30) modified nanoscale zero valent iron. *J. Hazard Mater.* 192, 44–53.
- Crowther, D.L., Dillard, J.G., Murray, J.W., 1983. The mechanisms of Co(II) oxidation on synthetic birnessite. *Geochim. Cosmochim. Acta* 47, 1399–1403.
- Dalmazio, I., Almeida, M.O., Augusti, R., Alves, T.M.A., 2007. Monitoring the degradation of tetracycline by ozone in aqueous medium via atmospheric pressure ionization mass spectrometry. *J. Am. Soc. Mass Spectrom.* 18, 679–687.
- Davies, J., Davies, D., 2010. Origins and evolution of antibiotic resistance. *Microbiol. Mol. Biol. Rev.* 74, 417–433.
- Delepee, R., Maume, D., Le Bizec, B., Pouliquen, H., 2000. Preliminary assays to elucidate the structure of oxytetracycline's degradation products in sediments – determination of natural tetracyclines by high-performance liquid chromatography–fast atom bombardment mass spectrometry. *J. Chromatogr. B* 748, 369–381.
- Drits, V.A., Silvester, E., Gorshkov, A.I., Manceau, A., 1997. Structure of synthetic monoclinic Na-rich birnessite and hexagonal birnessite.1. Results from X-ray diffraction and selected-area electron diffraction. *Am. Mineral.* 82, 946–961.
- Gao, J., Hedman, C., Liu, C., Guo, T., Pedersen, J.A., 2012. Transformation of sulfamethazine by manganese oxide in aqueous solution. *Environ. Sci. Technol.* 46, 2642–2651.
- Guo, X.J., Fujino, Y., Kaneko, S., Wu, K.G., Xia, Y.J., Yoshimura, T., 2001. Arsenic contamination of groundwater and prevalence of arsenical dermatosis in the Hetao plain area, Inner Mongolia, China. *Mol. Cell Biochem.* 222, 137–140.
- He, Y., Xu, J., Zhang, Y., Guo, C.S., Li, L., Wang, Y.Q., 2012. Oxidative transformation of carbamazepine by manganese oxides. *Environ. Sci. Pollut. Res.* 19, 4206–4213.
- Hu, X.G., Zhou, Q.X., Luo, Y., 2010. Occurrence and source analysis of typical veterinary antibiotics in manure, soil, vegetables and groundwater from organic vegetable bases, northern China. *Environ. Pollut.* 158, 2992–2998.
- Jeong, J., Song, W.H., Cooper, W.J., Jung, J., Greaves, J., 2010. Degradation of tetracycline antibiotics: mechanisms and kinetic studies for advanced oxidation/reduction processes. *Chemosphere* 78, 533–540.
- Ji, L.L., Wan, Y.Q., Zheng, S.R., Zhu, D.Q., 2011. Adsorption of tetracycline and sulfamethoxazole on crop residue-derived ashes: implication for the relative importance of black carbon to soil sorption. *Environ. Sci. Technol.* 45, 5580–5586.
- Jiao, S.J., Zheng, S.R., Yin, D.Q., Wang, L.H., Chen, L.Y., 2008. Aqueous photolysis of tetracycline and toxicity of photolytic products to luminescent bacteria. *Chemosphere* 73, 377–382.
- Ju, Y.M., Yang, S.G., Ding, Y.C., Sun, C., Zhang, A.Q., Wang, L.H., 2008. Microwave-assisted rapid photocatalytic degradation of malachite green in TiO₂ suspensions: mechanism and pathways. *J. Phys. Chem. A* 112, 11172–11177.
- Kummerer, K., 2009. Antibiotics in the aquatic environment – a review – Part I. *Chemosphere* 75, 417–434.
- Lafferty, B.J., Ginder-Vogel, M., Sparks, D.L., 2010a. Arsenite oxidation by a poorly crystalline manganese-oxide 1. Stirred-flow experiments. *Environ. Sci. Technol.* 44, 8460–8466.
- Lafferty, B.J., Ginder-Vogel, M., Zhu, M.Q., Livi, K.J.T., Sparks, D.L., 2010b. Arsenite oxidation by a poorly crystalline manganese-oxide. 2. Results from X-ray absorption spectroscopy and X-ray diffraction. *Environ. Sci. Technol.* 44, 8467–8472.
- Landrot, G., Ginder-Vogel, M., Livi, K., Fitts, J.P., Sparks, D.L., 2012. Chromium(III) oxidation by three poorly-crystalline manganese(IV) oxides. 1. Chromium(III)-oxidizing capacity. *Environ. Sci. Technol.* 46, 11594–11600.

- Li, J., Zhuang, G.S., Huang, K., Lin, Y., Xu, C., Yu, S.L., 2008. Characteristics and sources of air-borne particulate in Urumqi, China, the upstream area of Asia dust. *Atmos. Environ.* 42, 776–787.
- Liu, Y.K., Hu, J., Wang, J.L., 2014. Fe²⁺ enhancing sulfamethazine degradation in aqueous solution by gamma irradiation. *Radiat. Phys. Chem.* 96, 81–87.
- Lu, Z.J., Gan, J., 2013. Oxidation of nonylphenol and octylphenol by manganese dioxide: kinetics and pathways. *Environ. Pollut.* 180, 214–220.
- Lu, Z.J., Lin, K.D., Gan, J., 2011. Oxidation of bisphenol F (BPF) by manganese dioxide. *Environ. Pollut.* 159, 2546–2551.
- Ma, Y., Gao, N.Y., Li, C., 2012. Degradation and pathway of tetracycline hydrochloride in aqueous solution by potassium ferrate. *Environ. Eng. Sci.* 29, 357–362.
- Manning, B.A., Fendorf, S.E., Bostick, B., Suarez, D.L., 2002. Arsenic(III) oxidation and arsenic(V) adsorption reactions on synthetic birnessite. *Environ. Sci. Technol.* 36, 976–981.
- Mboula, V.M., Hequet, V., Gru, Y., Colin, R., Andres, Y., 2012. Assessment of the efficiency of photocatalysis on tetracycline biodegradation. *J. Hazard Mater.* 209, 355–364.
- Murray, J.W., 1974. Surface chemistry of hydrous manganese dioxide. *J. Colloid Interface Sci.* 19, 347–359.
- Ng, J.C., 2005. Environmental contamination of arsenic and its toxicological impact on humans. *Environ. Chem.* 2, 146–160.
- Pichler, T., Veizer, J., Hall, G.E.M., 1999. Natural input of arsenic into a coral reef ecosystem by hydrothermal fluids and its removal by Fe(III) oxyhydroxides. *Environ. Sci. Technol.* 33, 1373–1378.
- Post, J.E., 1999. Manganese oxide minerals: crystal structures and economic and environmental significance. *Proc. Natl. Acad. Sci. USA* 96, 3447–3454.
- Postma, D., Larsen, F., Hue, N.T.M., Duc, M.T., Viet, P.H., Nhan, P.Q., Jessen, S., 2007. Arsenic in groundwater of the Red River floodplain, Vietnam: controlling geochemical processes and reactive transport modeling. *Geochim. Cosmochim. Acta* 71, 5054–5071.
- Rodriguez-Lado, L., Sun, G., Berg, M., Zhang, Q., Xue, H., Zheng, Q., Johnson, C.A., 2013. Groundwater arsenic contamination throughout China. *Science* 341, 866–868.
- Rubert, K.F., Pedersen, J.A., 2006. Kinetics of oxytetracycline reaction with a hydrous manganese oxide. *Environ. Sci. Technol.* 40, 7216–7221.
- Sadiq, M., 1997. Arsenic chemistry in soils: an overview of thermodynamic predictions and field observations. *Water Air Soil Pollut.* 93, 117–136.
- Sassman, S.A., Lee, L.S., 2005. Sorption of three tetracyclines by several soils: assessing the role of pH and cation exchange. *Environ. Sci. Technol.* 39, 7452–7459.
- Seyler, P., Martin, J.M., 1990. Distribution of arsenite and total dissolved arsenic in major French estuaries – dependence on biogeochemical processes and anthropogenic inputs. *Mar. Chem.* 29, 277–294.
- Sorlini, S., Gialdini, F., 2010. Conventional oxidation treatments for the removal of arsenic with chlorine dioxide, hypochlorite, potassium permanganate and monochloramine. *Water Res.* 44, 5653–5659.
- Tani, Y., Miyata, N., Ohashi, M., Ohnuki, T., Seyama, H., Iwahori, K., Soma, M., 2004. Interaction of inorganic arsenic with biogenic manganese oxide produced by a Mn-oxidizing fungus, strain KR21-2. *Environ. Sci. Technol.* 38, 6618–6624.
- Tantuvay, L., Khan, F., 2004. Thermodynamic parameters and kinetic stability of manganese(II) complexes with some antibiotics: a polarographic approach. *Bull. Electrochem.* 20, 327–331.
- Tebo, B.M., Bargar, J.R., Clement, B.G., Dick, G.J., Murray, K.J., Parker, D., Verity, R., Webb, S.M., 2004. Biogenic manganese oxides: properties and mechanisms of formation. *Annu. Rev. Earth Planet. Sci.* 32, 287–328.
- Tournassat, C., Charlet, L., Bosbach, D., Manceau, A., 2002. Arsenic(III) oxidation by birnessite and precipitation of manganese(II) arsenate. *Environ. Sci. Technol.* 36, 493–500.
- Vartanian, V.H., Goolsby, B., Brodbelt, J.S., 1998. Identification of tetracycline antibiotics by electrospray ionization in a quadrupole ion trap. *J. Am. Soc. Mass Spectrom.* 9, 1089–1098.
- Villalobos, M., Toner, B., Bargar, J., Sposito, G., 2003. Characterization of the manganese oxide produced by *Pseudomonas putida* strain MnB1. *Geochim. Cosmochim. Acta* 67, 2649–2662.
- Yamamura, S., Watanabe, K., Suda, W., Tsuboi, S., Watanabe, M., 2014. Effect of antibiotics on redox transformations of arsenic and diversity of arsenite-oxidizing bacteria in sediment microbial communities. *Environ. Sci. Technol.* 48, 350–357.
- Yang, W.B., Zheng, F.F., Lu, Y.P., Xue, X.X., Li, N., 2011. Adsorption interaction of tetracyclines with porous synthetic resins. *Ind. Eng. Chem. Res.* 50, 13892–13898.
- Yu, K., Yang, S.G., He, H., Sun, C., Gu, C.G., Ju, Y.M., 2009. Visible light-driven photocatalytic degradation of Rhodamine B over NaBiO₃: pathways and mechanism. *J. Phys. Chem. A* 113, 10024–10032.
- Zhang, H.C., Huang, C.H., 2005. Oxidative transformation of fluoroquinolone antibacterial agents and structurally related amines by manganese oxide. *Environ. Sci. Technol.* 39, 4474–4483.
- Zhang, H., Ma, D.S., Hu, X.X., 2002. Arsenic pollution in groundwater from Hetao Area, China. *Environ. Geol.* 41, 638–643.
- Zhang, H.C., Chen, W.R., Huang, C.H., 2008. Kinetic modeling of oxidation of antibacterial agents by manganese oxide. *Environ. Sci. Technol.* 42, 5548–5554.
- Zhao, L., Dong, Y.H., Wang, H., 2010. Residues of veterinary antibiotics in manures from feedlot livestock in eight provinces of China. *Sci. Total Environ.* 408, 1069–1075.